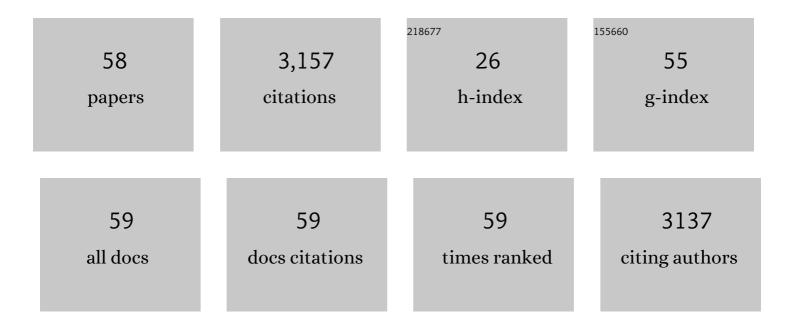
## Nancy M Washton

List of Publications by Year in descending order

Source: https://exaly.com/author-pdf/7010054/publications.pdf Version: 2024-02-01



#	Article	IF	CITATIONS
1	Effects of Si/Al ratio on Cu/SSZ-13 NH3-SCR catalysts: Implications for the active Cu species and the roles of BrÃ,nsted acidity. Journal of Catalysis, 2015, 331, 25-38.	6.2	341
2	Toward Rational Design of Cu/SSZ-13 Selective Catalytic Reduction Catalysts: Implications from Atomic-Level Understanding of Hydrothermal Stability. ACS Catalysis, 2017, 7, 8214-8227.	11.2	278
3	Effects of Alkali and Alkaline Earth Cocations on the Activity and Hydrothermal Stability of Cu/SSZ-13 NH <sub>3</sub> –SCR Catalysts. ACS Catalysis, 2015, 5, 6780-6791.	11.2	235
4	Effects of Systematic Methyl Substitution of Metal (III) Tris(n-Methyl-8-Quinolinolato) Chelates on Material Properties for Optimum Electroluminescence Device Performance. Journal of the American Chemical Society, 2001, 123, 6300-6307.	13.7	207
5	Synthesis and Evaluation of Cu-SAPO-34 Catalysts for Ammonia Selective Catalytic Reduction. 1. Aqueous Solution Ion Exchange. ACS Catalysis, 2013, 3, 2083-2093.	11.2	168
6	Synthesis and evaluation of Cu/SAPO-34 catalysts for NH3-SCR 2: Solid-state ion exchange and one-pot synthesis. Applied Catalysis B: Environmental, 2015, 162, 501-514.	20.2	166
7	Highly active electrolytes for rechargeable Mg batteries based on a [Mg <sub>2</sub> (î¼-Cl) <sub>2</sub> ] <sup>2+</sup> cation complex in dimethoxyethane. Physical Chemistry Chemical Physics, 2015, 17, 13307-13314.	2.8	126
8	Fe/SSZ-13 as an NH3-SCR catalyst: A reaction kinetics and FTIR/Mössbauer spectroscopic study. Applied Catalysis B: Environmental, 2015, 164, 407-419.	20.2	108
9	Sub-micron Cu/SSZ-13: Synthesis and application as selective catalytic reduction (SCR) catalysts. Applied Catalysis B: Environmental, 2017, 201, 461-469.	20.2	101
10	Unraveling the mysterious failure of Cu/SAPO-34 selective catalytic reduction catalysts. Nature Communications, 2019, 10, 1137.	12.8	99
11	A comparative kinetics study between Cu/SSZ-13 and Fe/SSZ-13 SCR catalysts. Catalysis Today, 2015, 258, 347-358.	4.4	94
12	NH3-SCR on Cu, Fe and Cu + Fe exchanged beta and SSZ-13 catalysts: Hydrothermal aging and propylene poisoning effects. Catalysis Today, 2019, 320, 91-99.	4.4	90
13	Transformation of Active Sites in Fe/SSZ-13 SCR Catalysts during Hydrothermal Aging: A Spectroscopic, Microscopic, and Kinetics Study. ACS Catalysis, 2017, 7, 2458-2470.	11.2	89
14	CRAGE enables rapid activation of biosynthetic gene clusters in undomesticated bacteria. Nature Microbiology, 2019, 4, 2498-2510.	13.3	85
15	Operando Solid-State NMR Observation of Solvent-Mediated Adsorption-Reaction of Carbohydrates in Zeolites. ACS Catalysis, 2017, 7, 3489-3500.	11.2	70
16	Revisiting effects of alkali metal and alkaline earth co-cation additives to Cu/SSZ-13 selective catalytic reduction catalysts. Journal of Catalysis, 2019, 378, 363-375.	6.2	59
17	Unraveling the Origin of Structural Disorder in High Temperature Transition Al <sub>2</sub> O <sub>3</sub> : Structure of Î,-Al <sub>2</sub> O <sub>3</sub> . Chemistry of Materials, 2015, 27, 7042-7049.	6.7	51
18	Evidence for Carbonate Surface Complexation during Forsterite Carbonation in Wet Supercritical Carbon Dioxide. Langmuir, 2015, 31, 7533-7543.	3.5	47

NANCY M WASHTON

#	Article	IF	CITATIONS
19	Self-organizing layers from complex molecular anions. Nature Communications, 2018, 9, 1889.	12.8	43
20	Nepheline crystallization in boron-rich alumino-silicate glasses as investigated by multi-nuclear NMR, Raman, & Mössbauer spectroscopies. Journal of Non-Crystalline Solids, 2015, 409, 149-165.	3.1	42
21	Measurement of the Reactive Surface Area of Clay Minerals Using Solid-State NMR Studies of a Probe Molecule. Journal of Physical Chemistry C, 2010, 114, 5491-5498.	3.1	41
22	Probing the molecular-level control of aluminosilicate dissolution: A sensitive solid-state NMR proxy for reactive surface area. Geochimica Et Cosmochimica Acta, 2008, 72, 5949-5961.	3.9	31
23	Protein–Mineral Interactions: Molecular Dynamics Simulations Capture Importance of Variations in Mineral Surface Composition and Structure. Langmuir, 2016, 32, 6194-6209.	3.5	31
24	Study of a Family of 40 Hydroxylated β-Cristobalite Surfaces Using Empirical Potential Energy Functions. Journal of Physical Chemistry C, 2007, 111, 5169-5177.	3.1	30
25	Abiotic Protein Fragmentation by Manganese Oxide: Implications for a Mechanism to Supply Soil Biota with Oligopeptides. Environmental Science & Technology, 2016, 50, 3486-3493.	10.0	30
26	A closed cycle for esterifying aromatic hydrocarbons with CO2 and alcohol. Nature Chemistry, 2019, 11, 940-947.	13.6	30
27	Effects of Al:Si and (AlÂ+ÂNa):Si ratios on the properties of the international simple glass, part II: Structure. Journal of the American Ceramic Society, 2021, 104, 183-207.	3.8	29
28	Quantification of Highâ€Temperature Transition Al <sub>2</sub> O <sub>3</sub> and Their Phase Transformations**. Angewandte Chemie - International Edition, 2020, 59, 21719-21727.	13.8	28
29	Chemical Trends in Solid Alkali Pertechnetates. Inorganic Chemistry, 2017, 56, 2533-2544.	4.0	26
30	Structural dependence of crystallization in glasses along the nepheline (NaAlSiO <sub>4</sub> ) ― eucryptite (LiAlSiO <sub>4</sub> ) join. Journal of the American Ceramic Society, 2018, 101, 2840-2855.	3.8	24
31	IRMOF-74( <i>n</i> )–Mg: a novel catalyst series for hydrogen activation and hydrogenolysis of C–O bonds. Chemical Science, 2019, 10, 9880-9892.	7.4	23
32	Unraveling the Dynamic Network in the Reactions of an Alkyl Aryl Ether Catalyzed by Ni/j³-Al <sub>2</sub> O <sub>3</sub> in 2-Propanol. Journal of the American Chemical Society, 2019, 141, 17370-17381.	13.7	23
33	Surface Interactions and Confinement of Methane: A High Pressure Magic Angle Spinning NMR and Computational Chemistry Study. Langmuir, 2017, 33, 1359-1367.	3.5	22
34	Structure and Chemistry in Halide Lead–Tellurite Glasses. Journal of Physical Chemistry C, 2013, 117, 3456-3466.	3.1	21
35	Quantitative Cu Counting Methodologies for Cu/SSZ-13 Selective Catalytic Reduction Catalysts by Electron Paramagnetic Resonance Spectroscopy. Journal of Physical Chemistry C, 2020, 124, 28061-28073.	3.1	20
36	Pulsed Field Gradient Nuclear Magnetic Resonance and Diffusion Analysis in Battery Research. Chemistry of Materials, 2021, 33, 8562-8590.	6.7	20

NANCY M WASHTON

#	Article	IF	CITATIONS
37	Remarkable self-degradation of Cu/SAPO-34 selective catalytic reduction catalysts during storage at ambient conditions. Catalysis Today, 2021, 360, 367-374.	4.4	18
38	Rate Controlling in Low-Temperature Standard NH <sub>3</sub> -SCR: Implications from <i>Operando</i> EPR Spectroscopy and Reaction Kinetics. Journal of the American Chemical Society, 2022, 144, 9734-9746.	13.7	17
39	Uranium Release from Acidic Weathered Hanford Sediments: Single-Pass Flow-Through and Column Experiments. Environmental Science & Technology, 2017, 51, 11011-11019.	10.0	15
40	Surprising formation of quasi-stable Tc( <scp>vi</scp> ) in high ionic strength alkaline media. Inorganic Chemistry Frontiers, 2018, 5, 2081-2091.	6.0	15
41	Probing Conformational Evolution and Associated Dynamics of Mg(N(SO <sub>2</sub> CF <sub>3</sub> ) <sub>2</sub> ) <sub>2</sub> A·Dimethoxyethane Adduct Using Solid-State <sup>19</sup> F and <sup>1</sup> H NMR. Journal of Physical Chemistry C, 2020, 124, 4999-5008.	3.1	13
42	Al <sub>2</sub> O <sub>3</sub> Atomic Layer Deposition on Nanostructured γ-Mg(BH <sub>4</sub> ) <sub>2</sub> for H <sub>2</sub> Storage. ACS Applied Energy Materials, 2021, 4, 1150-1162.	5.1	13
43	Methyl-Driven Overhauser Dynamic Nuclear Polarization. Journal of Physical Chemistry Letters, 2022, 13, 4000-4006.	4.6	13
44	NMR and IR Study of Fluorobenzene and Hexafluorobenzene Adsorbed on Alumina. Langmuir, 2007, 23, 5412-5418.	3.5	12
45	High-resolution microstrip NMR detectors for subnanoliter samples. Physical Chemistry Chemical Physics, 2017, 19, 28163-28174.	2.8	12
46	Effect of Acid on Surface Hydroxyl Groups on Kaolinite and Montmorillonite. Zeitschrift Fur Physikalische Chemie, 2018, 232, 409-430.	2.8	11
47	Mineral Surfaces as Agents of Environmental Proteolysis: Mechanisms and Controls. Environmental Science & Technology, 2019, 53, 3018-3026.	10.0	11
48	Theoretical Modeling of <sup>99</sup> Tc NMR Chemical Shifts. Inorganic Chemistry, 2016, 55, 8341-8347.	4.0	10
49	Spectroscopic Characterization of Aqua [ <i>fac</i> -Tc(CO) <sub>3</sub> ] <sup>+</sup> Complexes at High Ionic Strength. Inorganic Chemistry, 2018, 57, 6903-6912.	4.0	10
50	Monitoring solvent dynamics and ion associations in the formation of cubic octamer polyanion in tetramethylammonium silicate solutions. Physical Chemistry Chemical Physics, 2019, 21, 4717-4720.	2.8	9
51	Solid-state NMR examination of alteration layers on nuclear waste glasses. Journal of Non-Crystalline Solids, 2013, 369, 44-54.	3.1	8
52	Atomic-level studies of the depletion in reactive sites during clay mineral dissolution. Geochimica Et Cosmochimica Acta, 2012, 92, 100-116.	3.9	7
53	Conversion of nuclear waste to molten glass: Formation of porous amorphous alumina in a high-Al melter feed. Journal of Nuclear Materials, 2017, 483, 102-106.	2.7	7
54	High Temperature Acclimation of Leaf Gas Exchange, Photochemistry, and Metabolomic Profiles in <i>Populus trichocarpa</i> . ACS Earth and Space Chemistry, 2021, 5, 1813-1828.	2.7	7

#	Article	IF	CITATIONS
55	Role of a Multivalent Ion–Solvent Interaction on Restricted Mg <sup>2+</sup> Diffusion in Dimethoxyethane Electrolytes. Journal of Physical Chemistry B, 2021, 125, 12574-12583.	2.6	7
56	A novel high-temperature MAS probe with optimized temperature gradient across sample rotor for in-situ monitoring of high-temperature high-pressure chemical reactions. Solid State Nuclear Magnetic Resonance, 2019, 102, 31-35.	2.3	6
57	Interdisciplinary Round-Robin Test on Molecular Spectroscopy of the U(VI) Acetate System. ACS Omega, 2019, 4, 8167-8177.	3.5	5
58	Challenges and Solutions for Handling and Characterizing Alkali-Tc-Oxide Salts. MRS Advances, 2018, 3, 1191-1200.	0.9	1